Melting of a DNA Helix Terminus within the Active Site of a DNA Polymerase†

Remo A. Hochstrasser,‡,§ Theodore E. Carver,‡ Lawrence C. Sowers,‖ and David P. Millar*,‡

Department of Molecular Biology, The Scripps Research Institute, La Jolla, California 92037, and Division of Pediatrics, City of Hope National Medical Center, Duarte, California 91010

Received January 24, 1994; Revised Manuscript Received July 25, 1994®

ABSTRACT: Accurate synthesis of DNA by polymerases is due in part to the selective removal of misincorporated nucleotides by a 3′–5′ exonuclease activity (proofreading). Proofreading by an exonuclease domain containing a single-stranded DNA binding site may involve local melting of a duplex DNA substrate. Here we use time-resolved fluorescence spectroscopy to analyze the local melting of a DNA duplex terminus induced by the Klenow fragment of DNA polymerase I. Four oligodeoxynucleotide primer/templates were prepared, each containing the fluorescent adenine analog 2-aminopurine (A*) at the primer 3′ terminus, and one of the common DNA bases opposite the A* residue. Fluorescence decays of the duplex DNAs and the single primer oligonucleotide were jointly analyzed using global analysis procedures. Four lifetime components were resolved in the duplex DNAs, representing distinct conformational states of the terminal A* residue: paired A* bases, partially stacked A* bases, and extended A* bases. The variation of the apparent fraction of paired A* bases with temperature was in accord with optical melting data, and the extent of base pairing observed in each duplex was consistent with the base-pairing preferences of A* established in other studies. These results establish that the fluorescence decay characteristics of A* can be used to examine base-pairing interactions at a DNA duplex terminus. Since the fluorescence of A* can be observed without interference from protein amino acid residues, unlike existing methods for monitoring DNA melting transitions, this method was used to examine the extent to which Klenow fragment could induce fraying at each duplex terminus. Addition of D424A mutant Klenow fragment to the primer/template DNAs decreased the fraction of paired terminal bases and increased the fraction of extended terminal bases. These results demonstrate that Klenow fragment can melt a DNA duplex terminus, resulting in a population of DNA molecules in which the primer terminus is bound in an extended single-stranded conformation. The results of this study also establish a new method for examining base-pairing interactions within DNA molecules bound to proteins.

Replication of DNA by DNA polymerases is a process which occurs with high fidelity *in vivo*. The mechanisms by which fidelity is achieved have been the subject of a significant body of work. In prokaryotes, faithful replication involves selective incorporation of the correct base during the polymerization reaction, preferential extension of correctly paired primer termini, and selective removal of misincorporated nucleotides from the primer terminus by a separate 3′–5′ exonuclease activity of DNA polymerases (proofreading) [see Kunkel (1993) and Goodman et al. (1993) for reviews of recent work]. The molecular mechanisms that enable the enzyme to discriminate between correct and incorrect terminal base pairs are not well understood at present.

The Klenow fragment of DNA polymerase I from *Escherichia coli* is a useful model for understanding the molecular basis of polymerase fidelity mechanisms since it has been studied by a variety of structural (Ollis et al., 1985; Freemont et al., 1988; Beese et al., 1993), kinetic (Kuchta et al., 1988), genetic (Debyshire et al., 1988, 1991; Polesky et al., 1990), and spectroscopic approaches (Guest et al., 1991a). Crystallographic and genetic studies of Klenow fragment reveal that the active sites for the polymerase and 3′–5′ exonuclease reactions are located in separate structural domains of the enzyme, separated by about 25 Å (Ollis et al., 1985; Freemont et al., 1986; Derbyshire et al., 1988). The exonuclease site of the enzyme appears to only bind a single-stranded portion of a duplex DNA substrate, suggesting that melting of the DNA double helix is a prerequisite for exonuclease action (Freemont et al., 1988; Beese et al., 1993; Joyce & Steitz, 1987). The increased melting capacity of a mismatched duplex terminus could contribute to the selective removal of misincorporated nucleotides by the exonuclease activity of Klenow fragment.

Local melting of the DNA helix terminus within the exonuclease domain of Klenow fragment is consistent with the observation that 3′–5′ exonuclease activity on duplex DNA substrates increases markedly as temperature is increased (Brutlag & Kornberg, 1972). Moreover, biochemical experiments with covalently cross-linked DNA duplexes also indicate a requirement for strand separation during the 3′–5′ exonuclease reaction (Cowart et al., 1989). However, local melting of a DNA duplex terminus by a DNA polymerase has not been directly observed by a physical method under solution conditions. Melting transitions in DNA are usually monitored by the UV absorption of the bases. This method is based on the change in UV hypochromicity that is associated with the disruption of base-stacking interactions within the DNA double helix. However, hypochromicity measurements cannot be readily applied to DNA–protein complexes, since the near-UV absorption of aromatic amino acid residues overlaps the absorption band of the DNA bases. Base-pairing interactions in duplex DNA have also been studied using NMR spec-

† Supported by National Institutes of Health Grants GM44060 (to D.P.M.) and GM41336 (to L.C.S.).

* Author to whom correspondence should be addressed.

‡ The Scripps Research Institute.

§ Present address: Biophysikalische Chemie, Biozentrum, Klingelbergrstrasse 70, CH-4056 Basel, Switzerland.

‖ City of Hope National Medical Center.

® Abstract published in *Advance ACS Abstracts,* September 1, 1994.

0006-2960/94/0433-11971$04.50/0

troscopy (Sowers et al., 1986; Fazakerley et al., 1987), but the high molecular weight of DNA–polymerase complexes precludes the use of this technique for examining base-pairing interactions within the active sites of a polymerase.

Here we pursue an alternative spectroscopic approach for monitoring polymerase-induced melting of a DNA duplex terminus, based on the fluorescence emission of the adenine analog 2-aminopurine (A*). Several properties of A* make it suitable as a fluorescent probe of base-pairing interactions in duplex DNA molecules bound to proteins. First, A* can be conveniently introduced at a specific site in a DNA strand by standard oligonucleotide synthesis procedures. Second, although base-pair hydrogen bonding geometry is altered, A* is a realistic analog of adenine since it forms a Watson–Crick type base pair with thymine, thereby maintaining the B-form geometry of the DNA double helix (Sowers et al., 1986). In addition, A* can also mispair with other DNA bases. Third, fluorescence emission from A* can be selectively excited in the presence of the common DNA bases or protein tryptophan and tyrosine residues. Most importantly, the fluorescence lifetime of an A* base in DNA appears to be a sensitive reporter of base–base interactions (Nordlund et al., 1989; Guest et al., 1991b). Finally, A* is a mutagenic base *in vivo*, causing A·T ↔ G·C transitions (Ronen, 1979). This implies that once A* has been incorporated into a DNA strand by a polymerase, it can serve as a functional primer terminus during a subsequent round of nucleotide incorporation. Therefore, it is meaningful to study base-pairing interactions in the active sites of a polymerase using an A* base, and the results should also be relevant to the common DNA bases.

In the present study, we use time-resolved fluorescence spectroscopy to analyze the effect of base-pairing interactions on the fluorescence decay of an end terminal A* base in a DNA primer/template. We examine the fluorescence decay behavior of four primer/template duplexes in solution, each containing A* at the primer 3′ terminus and one of the common DNA bases opposite the A* residue. The multiexponential fluorescence decay behavior of A* observed in these DNAs is analyzed with a model based on ground-state conformational heterogeneity, wherein individual lifetime components are attributed to distinct conformational states of the A* base, including base-paired and unpaired states, and the pre-exponential factors are proportional to the population of each state. A similar analysis is carried out for the duplexes bound to Klenow fragment, yielding information on the distribution of conformational states of the primer terminus within the active sites of the enzyme. Binding of Klenow fragment to the DNA primer/templates is shown to cause a substantial loss of end terminal base pairs, resulting in a population of partially single-stranded molecules bound in an extended conformation. These observations are consistent with reported crystal structures of DNA bound at the exonuclease site of Klenow fragment, supporting the relevance of these structures to the DNA–protein complex present in solution under physiological conditions.

MATERIALS AND METHODS

Oligonucleotide Synthesis. Oligodeoxynucleotides were synthesized using a Pharmacia-Gene Assembler Plus using standard phosphoramidite chemistry. To synthesize oligonucleotides containing A* at the 3′ terminus (Figure 1), the protected synthon of A*, 5′-*O*-(dimethoxytrityl)-2-*N*-isobutyryl-2′-deoxynucleoside, was prepared (synthesis to be described elsewhere) and linked to a controlled-pore glass

```
5'  C G T C A G G C A A*        3'
3'  G C A G T C C G T X C A T A  5'

X = T, C, G, A
```

FIGURE 1: Oligonucleotide primer/templates used to examine base-pairing interactions at the primer 3′ terminus. A* is 2-aminopurine and X = T, C, G, or A.

solid support as described by Atkinson and Smith (1984). After synthesis, oligonucleotides were purified by HPLC using a polystyrene column (Trityl-on), followed by purification of the detritylated oligo by reverse-phase HPLC. All HPLC separations were performed using a gradient of acetonitrile in aqueous triethylammonium acetate.

The composition of the oligonucleotides was confirmed by two methods. Oligonucleotides were enzymatically digested with nuclease P1 (Sigma) and bacterial alkaline phosphatase (Sigma). The resulting deoxynucleosides were analyzed by reverse-phase HPLC using a spectral diode array detector. The presence of the expected deoxynucleosides was confirmed by their characteristic retention times and UV spectra, and integration of the HPLC chromatogram at selected wavelengths confirmed that the nucleosides were present in the correct molar ratios. The composition of the oligonucleotides was also confirmed by acid hydrolysis followed by GC/MS analysis.

DNA Polymerase. The mutant Klenow fragment containing the Asp^{424}–Ala substitution was isolated from *E. coli* CJ366 cells as described previously (Derbyshire et al., 1991). The CJ366 cells were kindly provided by C. Joyce. This mutant protein is devoid of measurable 3′–5′ exonuclease activity (Freemont et al., 1988), thereby ensuring that the DNA was not degraded during the course of the fluorescence measurements.

Duplex Formation. Duplexes were formed by mixing primer 10-mer (10 μM) and template 14-mer oligonucleotides (11 μM) in a buffer containing 50 mM Tris-HCl (pH 7.4), 100 mM NaCl, and 3 mM $MgCl_2$. A series of four duplexes contained all possible A*·X base pairs at the primer 3′ terminus, where X = T, C, A, and G in the template sequence (Figure 1). Each duplex contained a single-stranded overhang at the 5′ end of the template strand in order to favor binding to Klenow fragment in a unique orientation.

Formation of DNA–Protein Complexes. Complexes were formed by adding D424A Klenow fragment to the duplexes to a final concentration of 12 μM. Complete complexation of the DNA was confirmed by measuring the rotational correlation time of A* (Guest et al., 1991b). The slower rotational diffusion of the DNA–protein complex compared with the unbound DNA resulted in a large increase in the rotational correlation time upon binding. Titration of the DNAs with additional protein did not increase the rotational correlation time, indicating that all the DNA was bound to the protein.

Fluorescence Lifetimes. Samples were repetitively excited at 318 nm with the frequency-doubled output of a synchronously mode-locked and cavity-dumped CW dye laser (Coherent 702-CD). The pulse duration was less than 5 ps, and the pulse repetition frequency was 1.87 MHz. Fluorescence emission was collected at 90° to the excitation beam, passed through a polarizer oriented at 54.7° to the vertical excitation polarization, and focused on the slits of a 0.1 m single-grating monochromator (JY H-10). Fluorescence emission was monitored at 380 nm with a spectral bandpass of 4 nm. A microchannel plate photomultiplier (Hamamatsu R2809U-01) at the exit slit of the monochromator detected

the fluorescence, and its output was processed with a time-correlated single-photon counting system. The instrument response function, measured by scattering the laser pulses into the detector with a dilute suspension of nondairy coffee creamer, had a full width at half-maximum (FWHM) of 45 ps. Fluorescence decays were recorded in 512 channels with a time resolution of 36 ps/channel. Experiments were performed over a range of temperatures between 4 and 50 °C.

To resolve individual fluorescence lifetimes that are associated with distinct states of A* bases, the decay of fluorescence intensity was analyzed with a multiexponential model:

$$I(t) = g(t) \otimes K(t) \quad (1)$$

and

$$K(t) = \sum_{i=1}^{N} \alpha_i \exp(-t/\tau_i) \quad (2)$$

where $I(t)$ is the fluorescence intensity at time t after excitation, $K(t)$ describes the ideal decay of the fluorescence intensity, $g(t)$ is the instrument response function, $\otimes$ denotes convolution of two functions, α_i is the pre-exponential factor associated with each fluorescence lifetime τ_i, and N is the number of lifetime components. The parameters α_i and τ_i were optimized for the best fit of eqs 1 and 2 using a nonlinear least-squares method (Bevington, 1969). The quality of the fit was judged by the value of the reduced chi-square parameter, χ_r^2, and by examination of the weighted residuals. The minimum number of components required to fit the decay was determined empirically by incrementing N until χ_r^2 was close to 1.0 and the weighted residuals were randomly distributed about zero.

Fluorescence Lifetime Titrations. The primer oligonucleotide (Figure 1, 10 μM) was titrated with increasing amounts of template oligonucleotide (Figure 1), and the fluorescence decay of A* was measured after each addition. The resulting set of decay curves were globally analyzed according to eqs 1 and 2 by linking common lifetimes and optimizing the pre-exponential factors in each decay (Knutson et al., 1983). Global analysis was performed using the program TFIT, kindly provided by Dr. Ludwig Brand.

Optical Melting Measurements. The absorbance of the duplex DNAs was recorded at wavelengths of 275 and 330 nm in a 1 cm path length cuvette contained in a temperature-controlled housing. The duplex DNAs contained 4.5 μM primer and 5 μM template strands in the sample buffer mentioned above. The DNA solutions were heated at a rate of 1 °C/min, and the absorbance was recorded at 1 °C intervals.

RESULTS

Fluorescence Lifetimes of A Identify Distinct States of the Primer Terminus.* The steady-state emission spectrum and time-resolved fluorescence decay of the free primer oligonucleotide are shown in Figure 2. Formation of a duplex containing an A*·T base pair reduced the steady-state emission intensity of A* (Figure 2, upper panel) and resulted in a faster decay of fluorescence intensity (Figure 2, lower panel). Similar effects were observed with the other template strands (corresponding to X = C, G, and A opposite A*, Figure 1), although the magnitude of the changes was different in each case (not shown). These observations indicate that A* fluorescence is quenched within the duplex DNAs compared with the single-strand precursor.

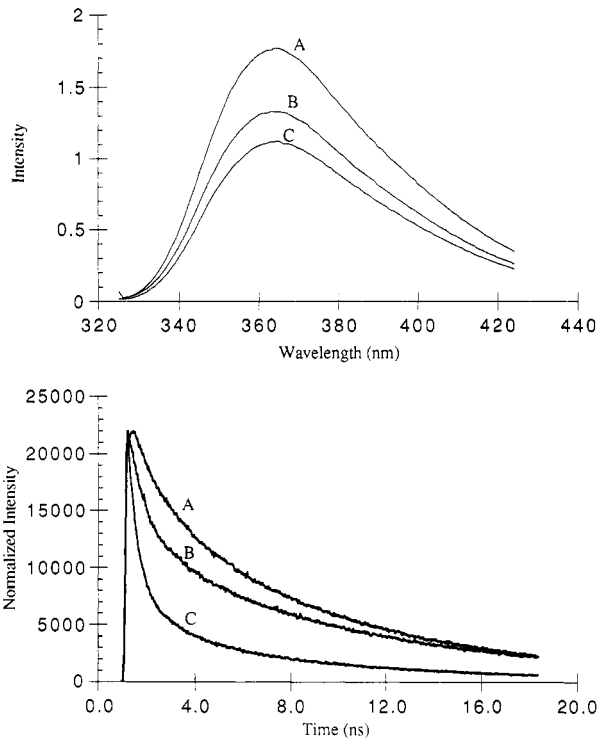

FIGURE 2: Steady-state fluorescence emission spectra and time-resolved fluorescence decays of A* in different states. Steady-state emission spectra (uncorrected) are shown in the upper panel and time-resolved fluorescence decays are shown in the lower panel for the same three samples. Data are shown for the primer oligonucleotide containing A* at the 3′ terminus (A); a primer/template containing A* at the primer 3′ terminus and thymine opposite the A* residue (C); and a complex of D424A Klenow fragment with the same primer/template (B). The base sequences of the primer and template oligonucleotides are shown in Figure 1 (X = T). Duplex samples contained 10 μM primer oligonucleotide and 11 μM template oligonucleotide. The complex contained 12 μM D424A Klenow fragment. All samples were prepared in a buffer of 50 mM Tris-HCl, pH 7.5, 100 mM NaCl, and 3 mM $MgCl_2$. Emission spectra and fluorescence decays were recorded at 4 °C.

Time-resolved fluorescence decays were analyzed in order to gain additional insight into the base–base interactions responsible for the differences in steady-state fluorescence intensity. The fluorescence decay of the free primer strand was fitted according to eqs 1 and 2 with three distinct lifetime components. The fit was excellent, as indicated by the reduced chi-square value (χ_r^2 = 1.05) and the absence of systematic deviations in the weighted residuals (not shown). However, the decay could not be adequately represented with fewer than three lifetimes. The three fluorescence lifetimes recovered from the best fit are listed in Table 1 together with the corresponding pre-exponential factors. Since the fluorescence decay of A* is intrinsically monoexponential (*e.g.*, A* monophosphate in aqueous solution has a 10 ns fluorescence lifetime; Rigler & Claesens, 1986; Guest et al., 1991b), these results indicate that the terminal A* base exists in at least three distinct states within the single-stranded primer oligonucleotide.

Attempts to fit the fluorescence decays of the duplex DNAs with three lifetimes were unsuccessful, as indicated by χ_r^2 values (1.4–1.6) and weighted residuals plots (Figure 3). However, excellent fits were obtained with four lifetimes, as shown by χ_r^2 values (1.03–1.15) and a random distribution of weighted residuals (Figure 3). Previous fluorescence decay studies of DNA duplexes containing A* in the center of the sequence also resolved four distinct lifetimes (Guest et al., 1991b). Three of the lifetimes recovered here for the duplex

Table 1: Fluorescence Lifetimes and Pre-Exponential Factors[a]

terminus[b]	state[c]	τ_1 (ps) (±50)	τ_2 (ns) (±0.20)	τ_3 (ns) (±0.30)	τ_4 (ns) (±0.5)	α_1 (±0.05)	α_2 (±0.05)	α_3 (±0.030)	α_4 (±0.030)
A*	free		0.39	1.95	9.1		0.17	0.273	0.557
A*	bound		0.30	2.47	12.7		0.10	0.056	0.844
A*·T	free	136	0.45	2.05	8.7	0.45	0.25	0.144	0.156
A*·C	free	139	0.56	1.97	8.8	0.39	0.22	0.244	0.146
A*·G	free	105	0.72	2.36	8.4	0.25	0.23	0.299	0.221
A*·A	free	159	0.72	2.56	8.7	0.17	0.28	0.297	0.253
A*·T	bound	133	0.48	2.20	11.1	0.23	0.29	0.143	0.337
A*·C	bound	127	0.60	2.39	10.0	0.25	0.21	0.214	0.326
A*·G	bound	125	0.59	2.54	10.4	0.20	0.10	0.170	0.530
A*·A	bound	172	0.89	2.90	9.5	0.12	0.19	0.274	0.416

[a] Errors in fluorescence lifetimes (τ) and pre-exponential factors (α) represent 95% confidence intervals. [b] The base pair at the primer 3′ terminus is indicated, except for the first two entries which are for the primer strand only. The complete base sequence of the primer and template strands is shown in Figure 1. [c] The primer/templates (10 μM primer strand, 11 μM template strand) were examined in 50 mM Tris buffer, pH 7.4, containing 100 mM NaCl and 3 mM $MgCl_2$ at 4 °C (free) or in the presence of D424A Knenow fragment (12 μM) in the same buffer at 4 °C (bound). The primer strand (10 μM) was examined in the same buffer at 4 °C, either alone (free) or in the presence of D424A Klenow fragment (45 μM) at 4 °C (bound).

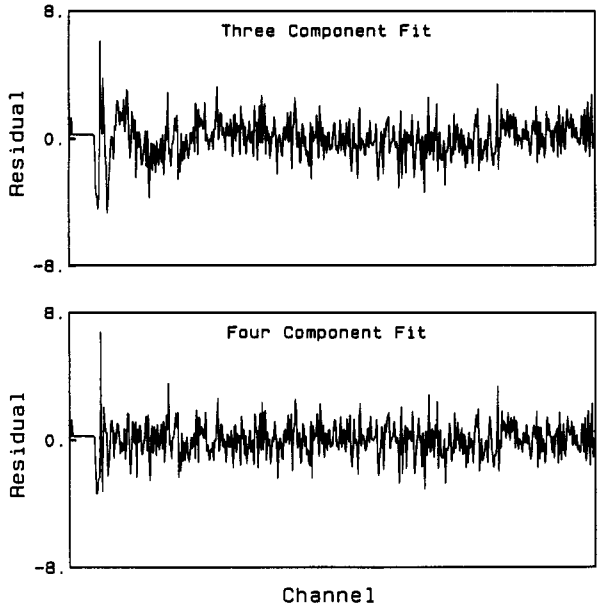

FIGURE 3: Weighted residuals obtained from fitting the fluorescence decay of A* in a primer/template duplex with either three or four lifetime components. The A* base at the primer 3′ terminus was opposite a thymine residue in the template strand. Complete base sequences of each strand are shown in Figure 1 (X = T). The fluorescence decay of A* is shown in Figure 2 (curve C, lower panel). The decay was fitted according to eqs 1 and 2 with either three or four lifetime components. The entire 512 channels of data were fitted, including the rising edge of the curve, which occurs around channel 30. The weighted residuals obtained for a three-component fit indicate the presence of systematic deviations between the fitted curve and the experimental decay. The weighted residuals are more randomly distributed for a four-component fit.

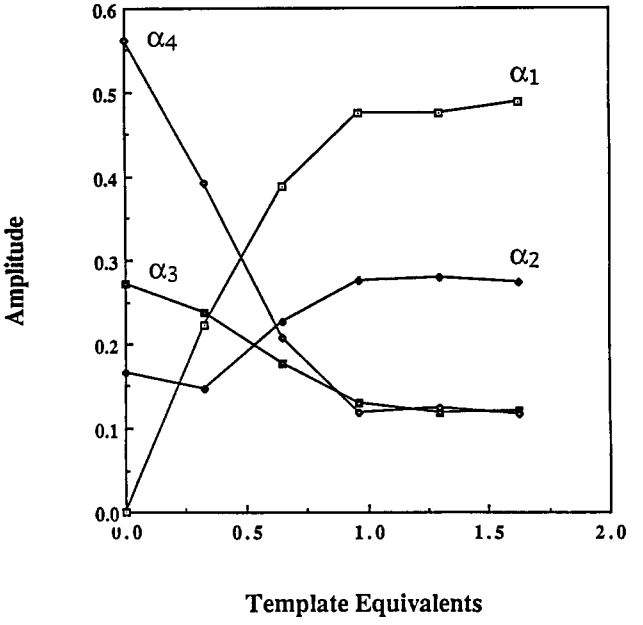

FIGURE 4: Global analysis of a fluorescence lifetime titration. Pre-exponential factors recovered for samples containing various molar ratios of primer and template oligonucleotides at 4 °C are shown. The primer strand contained A* at the 3′ terminus, and the template strand contained a thymine residue at the corresponding position. Complete base sequences of the oligonucleotides are shown in Figure 1 (X = T). The samples contained 10 μM primer oligonucleotide and various amounts of template oligonucleotide, as indicated by the x coordinate. The sample buffer contained 50 mM Tris-HCl, pH 7.4, 100 mM NaCl, and 3 mM $MgCl_2$. A common set of four lifetimes was used to describe the fluorescence decay in each sample according to eqs 1 and 2 (global $\chi_r^2 = 1.06$). The lifetimes are given in Table 1. The pre-exponential factor α_1 was set to zero in the sample containing no added template strand, since the corresponding lifetime was not detected in the fluorescence decay of the primer strand alone.

DNAs were similar to the decay times found for the free primer strand (Table 1), while a new lifetime between 100 and 150 ps was detected in the fluorescence decay of each duplex. Global analysis of a fluorescence lifetime titration was used to verify that some lifetime components were indeed common to both the single-strand and duplex DNAs. Starting with the primer strand alone, increasing amounts of a template strand (X = T in the template sequence, Figure 1) were added and the fluorescence decay was recorded after each addition. The template was added until there was no further change in the observed decay curve. In the samples containing less than one stoichiometric equivalent of the template strand, a mixture of duplex and free primer strands was present. The fluorescence decays of these samples thus represent a mixture of lifetime components characteristic of A* in both single-strand and double-strand DNAs. The set of fluorescence decay curves were globally analyzed according to eqs 1 and 2 by linking the lifetimes between each decay, while allowing the pre-exponential factors to vary for each curve. An excellent global fit was obtained with a common set of four lifetimes (global $\chi_r^2 = 1.06$). The lifetimes from the global analysis were essentially identical to those recovered from single-curve analysis of the fluorescence decay of the corresponding duplex DNA sample.

The pre-exponential factors recovered from the global analysis are shown in Figure 4. The shortest decay time, 136 ps, appears to be a property of duplex DNA only, since the amplitude of this lifetime component in the overall fluorescence decay increased as more duplex molecules were formed during

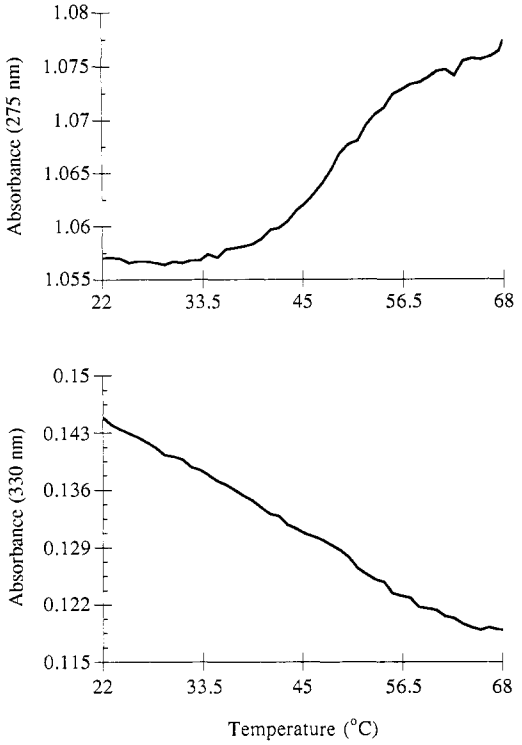

FIGURE 5: Optical melting curves of the primer/template containing an A*·T base pair (Figure 1) measured at 275 nm (upper panel) and 330 nm (lower panel). The sample contained 4.5 μM primer oligonucleotide and 5 μM template oligonucleotide in 50 mM Tris-HCl, pH 7.4, 100 mM NaCl, and 3 mM $MgCl_2$. Base sequences of the oligonucleotides are shown in Figure 1 (X = T). Melting curves were measured with a heating rate of 1 °C/min in a 1 cm path length cuvette.

the titration. In addition, this lifetime was not detected in the fluorescence decay of the free primer oligonucleotide, as noted previously. In contrast, the other three lifetime components (0.45 ns, 2.05 ns, and 8.7 ns) were present in all the titration samples, regardless of the relative amounts of the primer and template oligonucleotides, confirming that these lifetimes are common to both single-strand and duplex DNAs. We note that the presence of these lifetimes in duplex DNA samples did not simply reflect incomplete duplex formation, since the corresponding pre-exponential factors remained constant when an excess of the template strand was added to the primer strand (Figure 4). Therefore, the presence of decay times characteristic of A* bases in single-strand DNA must reflect a fraying of the duplex terminus.

The very short fluorescence lifetime that is observed in the primer/template DNAs presumably represents paired A* bases that are stacked into the double helix and hydrogen-bonded to the opposing residue in the template strand. NMR studies of A* bases in model DNA duplexes have shown that base pairing occurs between A* and thymine, cytosine, and adenine residues (Sowers et al., 1986; Fazakerley et al., 1987). The short fluorescence lifetime of the paired A* base could be due to π-stacking interactions between A* and neighboring bases in both strands of the duplex. Base-stacking interactions have previously been discussed as a mechanism for excited-state quenching in dinucleotides and nucleic acids (Barrio et al., 1973; Kubota et al., 1983; Wu et al., 1991). In addition, hydrogen-bonding interactions between A* and the opposing template residue might also facilitate the nonradiative decay of A*.

The three additional lifetimes in the fluorescence decay of each primer/template represent three unpaired states of the terminal A* base, as noted above. The longest fluorescence lifetime (8.4–8.7 ns) was similar to the lifetime of free A* bases in aqueous solution (10 ns), suggesting that this lifetime represents a melted state of the terminus in which the A* base is completely unstacked and extended into solution. The other two lifetimes (0.4–0.7 and 2.1–2.6 ns) are significantly shorter than the fluorescence lifetime of an isolated A* base, suggesting that these lifetimes represent melted states of the terminus in which the A* base is partially stacked with preceding primer bases. These states cannot be defined in precise structural terms, since the dependence of base-quenching interactions on geometrical factors is unknown at present.

Implicit in the lifetime assignments given above is that the multiexponential fluorescence decay behavior of the A* base reflects ground-state conformational heterogeneity. According to this model, the pre-exponential factor for each lifetime component is proportional to the relative population of each conformer, provided that the rate of interconversion between conformers is slow compared with the fluorescence decay rates. This condition should be fulfilled in the present system, since the rate of unstacking of DNA bases is slow on the fluorescence time scale (Wu et al., 1991). Thus, the pre-exponential factor for the shortest lifetime component (α_1) should be proportional to the fraction of paired A* bases in each primer/template. We examined the fluorescence decay of the primer/template containing an A*·T base-pair at several temperatures between 4 and 50 °C, to ascertain whether the apparent variation in α_1 reflected the melting of A*·T base pairs at higher temperatures. Melting of the A*·T base pair was also monitored by the 330 nm absorbance of the duplex, since there is a hypochromic change in absorbance at this wavelength as A* bases become unpaired (Eritja et al., 1986). The overall melting of the duplex was monitored by the 275 nm absorbance of the duplex.

The 275 nm absorbance profile of the duplex DNA showed a well-defined transition with a T_m value of 48 ± 2 °C (Figure 5). The 275 nm absorbance profiles were very similar for each duplex (not shown), and the T_m values were identical within experimental uncertainty, indicating that differences in the terminal base pair did not significantly influence the overall melting behavior of the duplexes. We note that the melting curves were measured with a duplex concentration of 5 μM, while the fluorescence experiments used a duplex concentration of 10 μM. Since T_m values for short DNA duplexes depend on the total strand concentration, the T_m values for the fluorescence samples will actually be higher than 48 °C. A comparison with optical melting data reported for oligonucleotides of similar length and at various strand concentrations (Aboul-ela et al., 1985) suggests that T_m will be 3–4 °C higher at the concentration used in the fluorescence measurements. The 330 nm absorbance of the duplex containing an A*·T base pair exhibited a gradual decrease with increasing temperature and showed no evidence of a discrete transition around the T_m value for overall melting of the duplex (Figure 5). Thus, the melting of the duplex terminus appears to be a progressive process rather than a cooperative transition. We note that cooperative melting transitions are observed for internal A*·T base pairs in DNA (Eritja et al., 1986).

The results of the fluorescence lifetime analysis at each temperature are presented in Table 2. Four lifetimes were required to fit the fluorescence decays at each temperature. The pre-exponential factor for the shortest lifetime (α_1) decreased gradually as temperature increased, in agreement with the 330 nm absorbance profile. In fact, the relative change

Table 2: Fluorescence Decay Parameters at Different Temperatures[a]

temp (°C)	τ_1 (ps) (±50)	τ_2 (ns) (±0.20)	τ_3 (ns) (±0.30)	τ_4 (ns) (±0.5)	α_1 (±0.05)	α_2 (±0.05)	α_3 (±0.030)	α_4 (±0.030)
4	136	0.45	2.05	9.1	0.45	0.25	0.144	0.156
10	116	0.58	2.62	9.1	0.45	0.24	0.132	0.178
20	125	0.65	2.54	8.3	0.40	0.28	0.143	0.177
30	129	0.62	2.51	7.4	0.31	0.28	0.210	0.200
40	114	0.60	2.58	7.5	0.17	0.34	0.313	0.177
50	178	0.64	2.65	7.6	0.12	0.32	0.361	0.199

[a] The fluorescence decay of a primer/template containing an A*·T base pair was recorded at each temperature and analyzed according to eqs 1 and 2. Errors represent 95% confidence intervals. The base sequences of the primer and template oligonucleotides are shown in Figure 1 (X = T).

in α_1 across the temperature range was comparable to the change in the 330 nm absorbance, suggesting that the two quantities are related. These results support the assignment of the shortest fluorescence lifetime component to paired A* bases. Table 2 also shows that the pre-exponential factors α_2 and α_3 increased as the temperature increased, with the largest change observed for α_3. The variation in these pre-exponential factors with increasing temperature reflects the increase in the population of unpaired A* bases as the duplex terminus is progressively melted. Interestingly, the pre-exponential factor α_4 did not vary significantly with temperature, implying that the fraction of extended A* bases remained constant between 4 and 50 °C.

The evidence presented above confirms that the pre-exponential factor α_1 is proportional to the equilibrium population of paired A* bases. However, α_1 is not precisely equal to the absolute fraction of paired A* bases, since the extinction coefficients of paired and unpaired A* bases are not equal at the laser excitation wavelength used in the fluorescence decay measurements, due to a spectral shift in the A* absorption maximum caused by base-pairing interactions (Eritja et al., 1986). Further fluorescence decay measurements at various excitation wavelengths are needed to establish the precise connection between the pre-exponential factors and the population of paired A* bases. Nevertheless, the apparent fraction of paired bases represented by α_1 contains information on the relative extent of base pairing at each duplex terminus. Moreover, a change in the relative population of end terminal base pairs, caused by binding of DNA polymerase, will be reflected in the value of α_1 recovered from the fluorescence lifetime analysis.

A lifetime between 100 and 150 ps was resolved in the fluorescence decay of each duplex in Figure 1, indicating that A* can pair to some extent with each of the common DNA bases (Table 1). However, the apparent fraction of paired A* bases was different in each duplex, which presumably reflects differences in the relative thermodynamic stability of the base pairs formed by A* with each of the common DNA bases. According to this criterion, the ranking in order of decreasing stability is as follows: A*·T > A*·C ≫ A*·G > A*·A. This ranking is consistent with other studies showing that A* forms stable base pairs with thymine and cytosine (Sowers et al., 1986). Moreover, the relative stability of the terminal base pairs implied by the fluorescence data is also consistent with the behavior of Klenow fragment in the presence of A*. Klenow fragment forms A*·T and A*·C base pairs in DNA with relatively high frequency, whereas purine–purine mispairs are rarely observed (Bessman et al., 1974; Watanabe & Goodman, 1981).

Since the fluorescence decays were analyzed in terms of four lifetime components, it is pertinent to consider whether the differences in α_1 values were significant in view of the uncertainty in these values caused by correlation between the fitted parameters. The 95% confidence limits listed in Tables 1 and 2 include the effect of parameter correlation. The differences in the α_1 values for the four duplexes are larger than the confidence limits, indicating that the apparent differences noted above are significant.

Melting of Helix Termini by Klenow Fragment. Binding of Klenow fragment to the duplex DNAs increased the steady-state fluorescence intensity of A* (Figure 2, upper panel) and resulted in a slower fluorescence decay compared with the free DNA (Figure 2, lower panel). The protein made no contribution to the observed fluorescence, since a sample containing only D424A Klenow fragment exhibited no fluorescence under the conditions of the present experiments (λ_{ex} = 318 nm, λ_{em} = 380 nm). Thus, the change in fluorescence upon binding of Klenow fragment to the DNAs specifically reflects changes in the environment of the A* base. The partial restoration of steady-state fluorescence intensity suggests that binding of Klenow fragment induced a loss of end terminal base pairs. This possibility was examined in greater detail by analyzing the fluorescence decays of the four DNA–protein complexes.

The fluorescence lifetime analysis showed that four lifetimes were required to adequately fit the fluorescence decays of all bound duplexes (χ_r^2 values in the range 1.05–1.15). The lifetime values were similar to those recovered for the unbound duplex DNAs, except for the longest lifetime component which was about 20–30% larger in the bound duplexes (Table 1). Likewise, binding of Klenow fragment to the primer strand alone also increased the longest lifetime, but had little effect on the two shorter lifetimes (Table 1). These results indicate that unstacked A* bases have a slightly longer fluorescence lifetime in the active site environment of Klenow fragment than in aqueous solution. However, the lifetimes that report on base–base interactions in the DNA were not significantly altered in the complexes, indicating that the protein environment did not perturb these interactions. Thus, the states of the A* base present in the free duplexes are probably present in the DNA–protein complexes. However, there may be additional nonfluorescent states of the A* base present in the complexes as well. This possibility is suggested by the observation that the increase in the integrated fluorescence intensity of A* following binding of Klenow fragment to the duplex DNAs was less than expected from the change in the average fluorescence lifetime, calculated from the fluorescence decay parameters (Table 1). Thus, Klenow fragment may cause static quenching in a subset of the A* bases.

The pre-exponential factor for the shortest lifetime component (α_1) was smaller for the bound duplex DNAs compared with the unbound DNAs, especially for the duplexes containing A*·T and A*·C base pairs. The decrease in α_1 reflects a smaller fraction of paired A* bases in the bound DNAs. For the duplexes containing A*·T and A*·C base pairs, the pre-exponential factor for the longest lifetime component (α_4) increased by a corresponding amount, while the remaining two pre-exponential factors exhibited little change upon

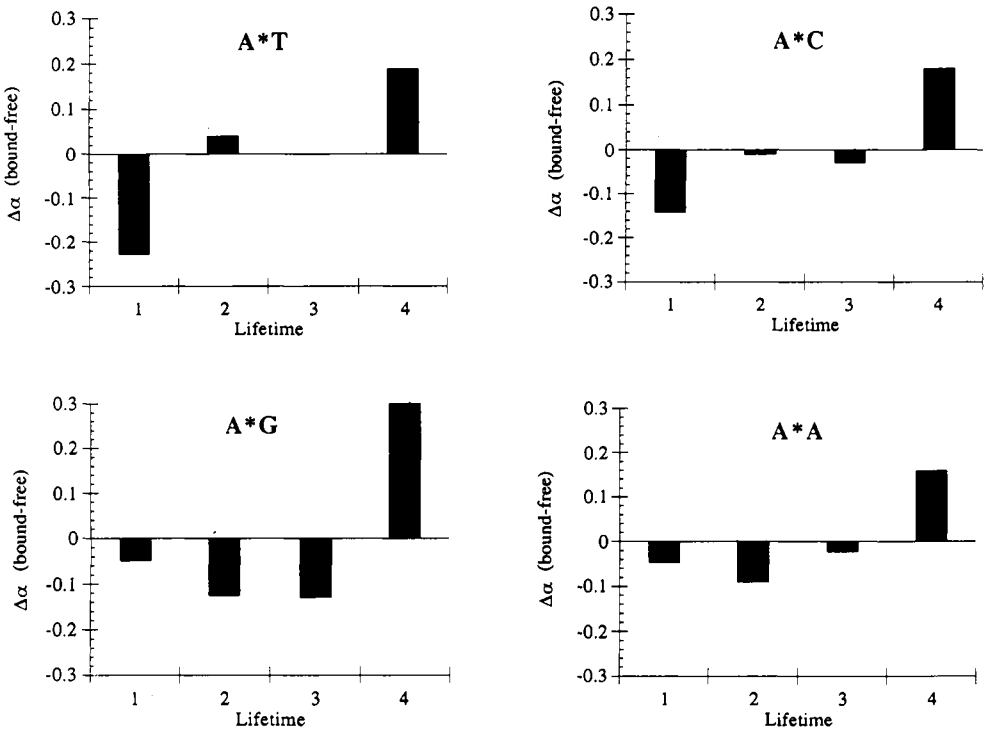

FIGURE 6: Changes in pre-exponential factors observed upon binding of Klenow fragment to four primer/template duplexes. The terminal base pair is indicated in each case. The complete base sequences of the primer and template oligonucleotides are given in Figure 1. The heights of the vertical bars are proportional to α_i(complex) − α_i(free), where the α_i values are the pre-exponential factors obtained from analysis of the fluorescence decay of the complex or free DNA. A negative bar indicates that the pre-exponential factor decreases upon binding of Klenow fragment to the DNA, while a positive bar indicates that the pre-exponential factor increases upon binding. The individual pre-exponential factors for the unbound primer/templates and complexes are given in Table 1.

binding of Klenow fragment to the DNAs (Figure 6, Table 1). These results indicate that A* bases which become unpaired within the enzyme are also completely unstacked and extended. On the basis of the relative change in α_1, the results in Table 1 indicate that between one-third and one-half of the A*·T and A*·C base pairs were disrupted upon binding of Klenow fragment to the DNAs. Thus, these data establish that binding of Klenow fragment caused a significant degree of melting of the duplex terminus in these DNAs.

Binding of Klenow fragment to duplexes containing A*·G and A*·A termini decreased the pre-exponential factor α_1 and increased α_4 (Table 1, Figure 6), again reflecting a decrease in the fraction of paired A* bases and an increase in the fraction of extended A* bases. However, the fraction of paired A* bases was already small in these duplexes, and the disruption in terminal base pairing caused by Klenow fragment was consequently less dramatic than observed with the A*·T and A*·C termini. Binding of Klenow fragment to the A*·G and A*·A termini also appeared to decrease the population of partially stacked A* bases (Table 1, Figure 6), an effect that was also observed when Klenow fragment bound to the primer strand alone. Overall, the effect of Klenow fragment on the conformational states of A* at A*·A and A*·G termini more closely resembled the behavior characteristic of a single-stranded terminus, which again underscores the observation that A* exhibits little tendency to form base pairs with guanine or adenine residues.

An alternative explanation for the increase in α_4 observed upon binding of Klenow fragment to all the DNAs is that some of the A* bases were excised from the primer strand, yielding a population of free A* bases in solution. The fluorescence lifetime of free A* bases is similar to the longest lifetime component of the A* base contained within DNA. Therefore, it was important to ensure that residual exonuclease activity of the D424A mutant enzyme did not affect the results obtained for the DNA–protein complexes. To check whether any exonucleolysis had occurred during the fluorescence decay measurement, EDTA (5 mM) was added afterward to remove magnesium from the enzyme and thereby stop any further exonucleolysis from occurring. The fluorescence decay was then measured a second time and compared with data obtained for a freshly prepared complex containing EDTA and no added magnesium. Any difference between the decays measured for these two control samples would indicate that an irreversible reaction had occurred during the original fluorescence measurement in the presence of magnesium. However, the decays were identical, confirming that the amount of exonucleolysis occurring during the decay measurements in the presence of magnesium was too small to affect the results.

DISCUSSION

Direct observation of local melting of the DNA double helix by a DNA polymerase under solution conditions has been hindered by the lack of a suitable physical method for probing base-pairing interactions in DNA molecules bound to proteins. Observation of DNA melting transitions based on measurements of UV absorbance is complicated by the overlapping UV absorption of aromatic amino acid residues in the polymerase, while the high molecular weight of DNA–polymerase complexes precludes the use of NMR spectroscopy for examining local melting of a duplex terminus within the active site of a DNA polymerase. In the present study, we have examined the potential of using the base analog 2-aminopurine (A*) as a fluorescent probe of base-pairing interactions in DNA. This base analog is closely related to adenine, while its spectral properties are distinct from the common DNA bases or aromatic amino acids tryptophan and tyrosine, thereby enabling fluorescence measurements to be

carried out in the presence of a DNA polymerase. The fluorescence intensity of an A* base in double-strand DNA is reduced in comparison with the corresponding single-strand precursor, suggesting that the excited-state decay of A* is influenced by base-pairing interactions within the DNA double helix.

The quenching of A* resulting from base-pair formation was directly established by analyzing the time-resolved fluorescence decay of a terminal A* base in four primer/template duplexes, in which A* was paired with each of the common DNA bases. The fluorescence lifetime analysis resolved the A* base at each duplex terminus into four distinct states. The shortest lifetime component (100–150 ps) appears to represent a population of A* bases that are stacked into the double helix and paired with the opposing template base. This assignment is supported by three lines of evidence. First, the 100–150 ps lifetime was only observed when both primer and template strands were present. Second, the pre-exponential factor associated with this lifetime (α_1), which is proportional to the fraction of paired A* bases, decreased with increasing temperature in a manner that parallels the 330 nm absorbance profile, which specifically reports on pairing of the A* base in the duplex DNAs in solution. Finally, the relative extent of base pairing of A* with each of the common bases, reflected in the relative α_1 values, correctly predicts the greater stability of A*·T and A*·C base pairs compared with A*·G and A*·A pairs.

In addition to the paired state, the fluorescence lifetime analysis has revealed three unpaired states of the terminal A* base in each duplex. The existence of these states reflects fraying of the duplex terminus in solution. One of these unpaired states has a fluorescence lifetime that is similar to that of a free A* base in aqueous solution, demonstrating that this lifetime represents a fully unstacked and extended terminal base. The two remaining unpaired states of the primer terminus have lifetimes that are shorter than an isolated A* base, suggesting that these states involve a partial stacking of the terminal A* residue with preceding bases in the primer strand. Melting of the duplex terminus in solution does not appear to result in fully extended A* bases, but rather promotes formation of unpaired A* bases that remain in proximity to preceding bases in the primer strand. Formation of a completely unstacked and extended terminal base appears to be unfavored in solution.

To establish that the present method can be used to examine base-pairing interactions at a duplex terminus in a DNA–polymerase complex, we have examined the fluorescence decay of the four primer/template duplexes bound to an exonuclease-deficient D424A mutant Klenow fragment. The fluorescence lifetime data obtained for the free DNAs indicate that the duplexes containing A*·T and A*·C base pairs are the best models for examining polymerase-induced melting, since these DNAs exhibit the highest fraction of paired termini prior to addition of the enzyme. The fluorescence lifetime data obtained for the complexes confirm that the distinct populations of paired and unpaired A* bases can still be detected in the presence of Klenow fragment. On the basis of the observed changes in the pre-exponential factors, which reflect the relative amounts of each conformational state of A*, it is apparent that binding of Klenow fragment to these DNAs reduces the population of paired A* bases and increases the population of extended A* bases by a corresponding amount (Figure 6). These results establish that binding of Klenow fragment to duplex DNA causes a substantial loss of end terminal base pairs. Although our data do not indicate the precise fraction of paired A* bases in either the bound or unbound DNAs, the relative change in the apparent fraction of paired bases (α_1) is significant. It is especially noteworthy that binding of Klenow fragment caused significant fraying of the duplex terminus at a temperature of 4 °C, whereas in solution the temperature had to be increased to almost 40 °C to effect a comparable reduction in the apparent fraction of paired A* bases (Table 1). However, Klenow-induced melting appears to be fundamentally different from the thermal melting observed in solution, since Klenow results in completely unstacked and extended A* bases, whereas melting of the duplex terminus in solution yields A* bases that remain partially stacked with preceding primer bases, as noted above. We also note that Klenow fragment did not disrupt the terminal base pair in every bound DNA molecule, since the shortest lifetime component was still detectable in the complexes.

The preferential formation of extended terminal A* residues upon binding of Klenow fragment to the primer/templates is consistent with crystallographic studies showing that the primer terminus of a duplex DNA substrate binds at the exonuclease site of the enzyme in an extended single-stranded conformation. The cocrystal structure of duplex DNA and Klenow fragment reveals four single-stranded nucleotides bound in an extended conformation, with a leucine side chain (Leu-361) of the protein wedged between the 3′ terminal and penultimate nucleotides (Freemont et al., 1988). Furthermore, a dT_4 tetranucleotide cocrystallized with Klenow fragment was observed to bind in the exonuclease site in a similar conformation (Freemont et al., 1988). The mode of DNA binding observed in these cocrystal structures can account for the increased fraction of extended A* bases that is observed when Klenow fragment binds to the primer/template duplexes or the primer strand alone. The extended conformation of the sugar–phosphate backbone and the intervening leucine residue would prevent stacking of A* with the preceding nucleotide and thereby increase the fraction of A* residues that exhibit the fluorescence lifetime characteristic of an isolated A* base (Table 1). Therefore, the decrease in paired A* bases and the corresponding increase in extended A* bases that we observe by fluorescence lifetime measurements are consistent with binding of the frayed duplex terminus at the exonuclease site of the enzyme. Our results support the relevance of the cocrystal structure of Klenow fragment bound to duplex DNA to the complex present in solution under physiological conditions.

Fluorescence anisotropy decay experiments with dansyl-labeled DNA duplexes bound to Klenow fragment have shown that the DNA primer terminus is partitioned between the polymerase and exonuclease sites of the enzyme (Guest et al., 1991a). Using this technique, we have recently examined a series of different primer/templates bound to D424A Klenow fragment, to determine how the local base sequence of the terminus influences the distribution of DNA between the polymerase and exonuclease domains of the enzyme (Carver et al., 1994). Single base mismatches at the primer terminus caused a large increase in the equilibrium partitioning of DNA into the exonuclease site, while DNA containing two or more consecutive terminal mismatches was bound exclusively at the exonuclease site (Carver et al., 1994). In addition, A·T-rich sequences promoted binding of the DNA terminus at the exonuclease site (Carver et al., 1994). The sequences that were found to increase binding at the exonuclease site are sequences that are expected to destabilize the duplex terminus and facilitate local melting, suggesting that the primer terminus binds to the exonuclease site as a frayed end. Thus, the

partitioning experiments with dansyl-labeled DNA are completely consistent with the results of the present study, in which melting of the duplex terminus by Klenow fragment is directly manifested in the fluorescence characteristics of the end terminal A* base. This suggests that a correlation may exist between the fraction of extended terminal bases detected by A* fluorescence and the fraction of DNA bound at the exonuclease site of the enzyme. If so, duplexes containing A*·G and A*·A termini must have a greater tendency to bind at the exonuclease site than duplexes containing A*·T and A*·C termini, since these DNAs show the largest α_4 values when bound to Klenow fragment (Table 1). This is consistent with the partitioning measurements, which show that primer termini containing mismatched terminal base pairs have a greater tendency to bind at the exonuclease site than DNAs containing more stable base pairs (Carver et al., 1994).

An exonuclease-deficient D424A mutant Klenow fragment derivative was used in this study to prevent degradation of the DNA during the fluorescence measurements. Thus, it is important to consider the relevance of our results to the behavior of the native enzyme, since the D424A mutant might interact differently with DNA. The crystal structure of D424A Klenow fragment has been solved and compared with the structure of the wild-type enzyme (Derbyshire et al., 1988). The two structures are identical, except for the modified amino acid residue and the absence of a magnesium cation at the exonuclease site of the enzyme. The missing magnesium cation has been implicated as being essential for catalysis of the 3′-5′ exonuclease reaction (Derbyshire et al., 1988). Since the overall structures of the mutant and wild-type enzymes are identical, it is very likely that they bind DNA in a similar manner. Time-resolved fluorescence anisotropy measurements with dansyl-labeled DNA also confirm that D424A Klenow fragment can bind DNA at both the polymerase and 3′-5′ exonuclease active sites in a similar manner to that of the wild-type enzyme (Carver et al., 1994).

CONCLUSIONS

In this paper, we have demonstrated that the fluorescence decay characteristics of an A* base can be used to monitor base-pairing interactions and local melting at a DNA duplex terminus. Moreover, this method can be used to examine base-pairing interactions in duplex DNA molecules bound to proteins. Analysis of the fluorescence decay of A* using a discrete lifetime model yields information on distinct conformational states of this base in DNA, including paired and unpaired states. The results of this analysis indicate that A* has a propensity for forming stable base pairs with thymine and cytosine, in agreement with other studies of this mutagenic base. Binding of Klenow fragment to DNA containing these base pairs at the duplex terminus decreased the fraction of paired A* bases, resulting in an increased population of extended and completely unstacked terminal bases. The results of this study establish that Klenow fragment substantially disrupts base pairing at a duplex terminus and are in accord with models which invoke melting as a key step in the proofreading mechanism of the enzyme. The method described here for examining base-pairing interactions in DNA is not limited to polymerases, however. For example, such methods could be used to monitor any enzymatic process that produces single-stranded DNA from duplex DNA precursors, or vice versa.

REFERENCES

Abou-ela, F., Koh, D., Tinoco, I., & Martin, F. H. (1985) *Nucleic Acids Res. 13*, 4811–4824.

Allen, D. J., Darke, P. L., & Benkovic, S. J. (1989) *Biochemistry 28*, 4601–4607.

Atkinson, T., & Smith, M. (1984) in *Oligonucleotide Synthesis, a Practical Approach* (Gait, M. J., Ed.) pp 35–81, IRL Press, Washington.

Barrio, J. R., Tolman, G. L., Leonard, L. J., Spencer, R. D., & Weber, G. (1973) *Proc. Natl. Acad. Sci. U.S.A. 70*, 941–943.

Beese. L., Derbyshire, V., & Steitz, T. A. (1993) *Science 260*, 352–355.

Bessman, M. J., Muzyczka, N., Goodman, M. F., & Schnaar, R. L. (1974) *J. Mol. Biol. 88*, 409–421.

Bevington, P. R. (1969) *Data Reduction and Error Analysis for the Physical Sciences*, McGraw-Hill, New York.

Brutlag, D., & Kornberg, A. (1979) *J. Biol. Chem. 247*, 241–248.

Carver, T. E., Hochstrasser, R. A., & Millar, D. P. (1994) *Proc. Natl. Acad. Sci. U.S.A.* (in press).

Cowart, M., Gibson, K. J., Allen, D. J., & Benkovic, S. J. (1989) *Biochemistry 28*, 1975–1983.

Derbyshire, V., Freemont, P. S., Sanderson, M. R., Beese, L., Friedman, J. M., Joyce, C. M., & Steitz, T. A. (1988) *Science 240*, 199–201.

Derbyshire, V., Grindley, N. D. F., & Joyce, C. M. (1991) *EMBO J. 10*, 17–24.

Eritja, R., Kaplan, B. E., Mhaskar, D., Sowers, L. C., Petruska, J., & Goodman, M. F. (1986) *Nucleic Acids Res. 14*, 5869–5884.

Fazakerley, G. V., Sowers, L. C., Eritja, R., Kaplan, B. E., & Goodman, M. F. (1987) *Biochemistry 26*, 5641–5646.

Freemont, P. S., Ollis, D. L., Steitz, T. A., & Joyce, C. M. (1986) *Proteins 1*, 66–73.

Freemont, P. S., Friedman, J. M., Beese, L. S., Sanderson, M. R., & Steitz, T. A. (1988) *Proc. Natl. Acad. Sci. U.S.A. 85*, 8924–8928.

Goodman, M. F., Creighton, S., Bloom, L. B., & Petruska, J. (1993) *Crit. Rev. Biochem. Mol. Biol. 28*, 83–126.

Guest, C. R., Hochstrasser, R. A., Dupuy, C. G., Allen, D. J., Benkovic, S. J., & Millar, D. P. (1991a) *Biochemistry 30*, 8759–8770.

Guest, C. R., Hochstrasser, R. A., Sowers, L. C., & Millar, D. P. (1991b) *Biochemistry 30*, 3271–3279.

Joyce, C. M., & Steitz, T. A. (1987) *Trends Biochem. Sci. 12*, 288–292.

Knutson, J. R., Beechem, J. M., & Brand, L. (1983) *Chem. Phys. Lett. 102*, 501–507.

Kubota, Y., Motoda, Y., Fujisaki, Y., & Steiner, R. F. (1983) *Biophys. Chem. 18*, 225–232.

Kunkel, T. A. (1993) *J. Biol. Chem. 267*, 18251–18254.

Nordlund, T. M., Andersson, S., Nilsson, L., Rigler, R., Graslund, A., & McLaughlin, L. W. (1989) *Biochemistry 28*, 9095–9103.

Ollis, D. L., Brick, P., Hamlin, R., Xuong, N. G., & Steitz, T. A. (1985) *Nature 313*, 762–766.

Polesky, A. H., Steitz, T. A., Grindley, N. D. F., & Joyce, C. M. (1990) *J. Biol. Chem. 265*, 14579–14591.

Rigler, R., & Claesens, F. (1986) in *Structure and Dynamics of RNA* (van Knippenberg, P. H., & Hilbers, C. W., Eds.) pp 45–54, Plenum Press, New York.

Ronen, A. (1979) *Mutat. Res. 75*, 1–47.

Sowers, L. C., Fazakerley, G. V., Eritja, R., Kaplan, B. E., & Goodman, M. F. (1986) *Proc. Natl. Acad. Sci. U.S.A. 83*, 5434–5438.

Watanabe, S. M., & Goodman, M. F. (1981) *Proc. Natl. Acad. Sci. U.S.A. 78*, 2864–2868.

Wu, P., Nordlund, T. M., Gildea, B., & McLaughlin, L. W. (1990) *Biochemistry 29*, 6508–6514.